

Internal Electron Diffraction from Atomically Ordered Subsurface Nanostructures in Metals

O. Kurnosikov, H. J. M. Swagten, and B. Koopmans

Department of Applied Physics, cNM, Eindhoven University of Technology, 5600MB Eindhoven, The Netherlands
(Received 7 May 2010; revised manuscript received 1 March 2011; published 12 May 2011)

We demonstrate that a part of interface at a subsurface nanocavity in Cu(110) can efficiently induce electron scattering back to the surface even if it is inclined with respect to the surface, if the condition for electron diffraction is fulfilled. This backscattering induces oscillations of electron local density of states at the surface versus electron energy. In agreement with our model calculations, the diffraction is assigned to a specific atomic structure at the interface, and is found to be significantly enhanced by focussing of electron waves for propagation along the [110] direction.

DOI: [10.1103/PhysRevLett.106.196803](https://doi.org/10.1103/PhysRevLett.106.196803)

PACS numbers: 73.21.Fg, 05.70.Ln, 68.37.Ef, 72.10.Fk

Recently, it has been shown that a bulk subsurface impurity can induce spatial oscillations of electron local density of states (LDOS), as observed at a surface with scanning tunneling microscopy-spectroscopy (STM/STS) [1]. These 3D oscillations of LDOS are similar to the LDOS oscillations around a surface impurity, which have been scrutinized for 2D electron systems [2]. In analogy with an advanced 2D system such as a quantum corral [3], it would be also expected that a *structured* ensemble of bulk scattering centers may remarkably modify the scattering, enhancing the LDOS oscillations in some locations or in some directions. However, the lack of accessibility to buried atomic structures makes such an experiment almost unfeasible. Nevertheless, a simple ensemble of scattering centers can be built up by segregation of impurities resulting in buried nanoclusters with nanofacets or atomically ordered interface. These nanoclusters reveal a pattern of electron backscattering that remarkably differs from scattering on a single bulk impurity [4,5]. In such a case of scattering from a buried object, the reflection from a nanofacet *parallel* to the surface induces localized quantum well (QW) resonances [4–7], which are in principle the same as the delocalized QW resonances observed in a thin film system [8]. Scattering or reflection from other *inclined* facets or *inclined* interfaces would naively be expected to result only in a very weak spatial oscillation of LDOS, similar to scattering on a single atom, but not forming any QW resonances [7].

In this Letter we will demonstrate that if such an inclined interface is atomically *structured*, under appropriate conditions the *diffraction* of electrons can induce an enhanced scattering of electron waves back to the surface. Even if the structured interface is buried several nanometers below a surface, the diffraction effect can lead to the observation of resonances that are similar to QW resonances induced by reflections from a flat parallel nanofacet. It will be shown that such a possibility can be realized for a metallic system displaying particular bulk electronic properties and a specific interface structure.

In the present work we investigate the electron scattering from faceted Ar-filled nanocavities [4–7] buried several nanometers below a Cu(110) surface. In this system we observe simultaneously two kinds of resonances: (i) QW resonances formed by the reflection of electrons from the upper parallel flat facet of the nanocavity, which is consistent with previous observations [4–6], and (ii) the initially unexpected resonances originating, as shown later, from electron *diffraction* from the interface at the sides of the nanocavity. This inclined interface is intrinsically nanostructured by atomic chains, inducing diffraction of electrons back to the probing point. The intensity and sharpness of the effect are greatly enhanced by exploiting the phenomenon of electron focusing [1,9–14], which in copper is very efficient along the $\langle 110 \rangle$ direction. We developed a model describing this system and did the simulation elucidating the role of the diffraction process.

The subsurface nanocavities were formed by annealing of the Cu(110) sample containing implanted argon. Although the shape of nanocavities [4–7], built mostly by three types of atomically flat facets, {110}, {111}, and {001}, is governed by anisotropy of the surface energy of copper, the exact size and shape is not well defined and may depend on the procedure of sample preparation described in detail previously [6]. The kind of noble gas is of no remarkable influence on the shape, structure and electronic properties of interface [7]. The choice of crystal orientation allows us to profit from the anisotropy of electronic properties resulting in the focusing effect which concentrates the electron transport to a large extent along the $\langle 110 \rangle$ direction. A surface differential conductance (SDC) versus electron energy in a chosen location, as well as mapping SDC at fixed energy across the surface, is measured by the STM/STS technique [Fig. 1(a)] at 77 K.

The distribution of SDC across the Cu(110) surface above the subsurface nanocavities reveals a rich variety of spots different in size and shape [Fig. 1(b)]. The intensity of the measured signal within the spots corresponds to the deviation of SDC from its mean value, and is found to

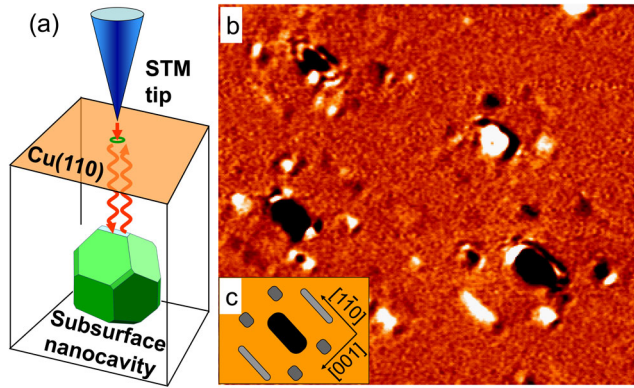


FIG. 1 (color online). (a) Scheme of the experiment. (b) Differential conductance map ($46.5 \times 42 \text{ nm}^2$) measured at 400 mV and showing many spots of deviating conductance across the surface induced by subsurface nanocavities. (c) Schematic drawing of the group of spots appearing together in (b).

vary quasiperiodically with the bias voltage. After closer inspection it can be noticed that the relative position of the spots is not completely random. In spite of the various size and shape of the spots as well as difference in the value of SDC [Fig. 1(b)], a systematic pattern emerges consisting of a big elongated spot surrounded by several smaller satellite spots in a symmetric way as schematically shown in Fig. 1(c). Usually, four small spots are observed on distances of 3–5 nm from the ends of the central spot. Additionally, two elongated satellite spots lie at both sides of the central spot [Fig. 2(a)] parallel to the $[1\bar{1}0]$ direction.

Considering only the central spot, its origin is obvious and can be explained by a QW formation between the (110) surface and parallel upper (110) facet reflecting the electrons back [4–6]. Indeed, the observed central spot is always elongated and oriented in the same way as expected for the upper (110) facet of the nanocavity [Fig. 2(b)]. The oscillation of SDC as a function of bias voltage within the central spot determines the depth of the upper (110) facet [4–6]. The SDC oscillation, induced by a particular nanocavity, is presented in Fig. 2(a) and 2(c). For this case, the depth is found to be 6 nm, while measurements for other nanocavities indicate a spread of depths between 2 and 10 nm. The presence of the extra satellite spots is less trivial to explain. They display another oscillation period [Fig. 2(c), plots 2–4], which cannot be attributed to the (110) facet.

The origin of the satellite spots becomes clear by analyzing the lateral position of these spots together with their oscillation period when measuring SDC versus energy. Regarding the Cu(110) sample, the bulk electron states probed by the STM tip should mainly correspond to the direction perpendicular to the surface due to both the focusing effect favoring the $\langle 110 \rangle$ direction and the k -vector selection rule applied for the tunneling electrons. To prove this, an analysis of the ratio s/δ of distances s between the

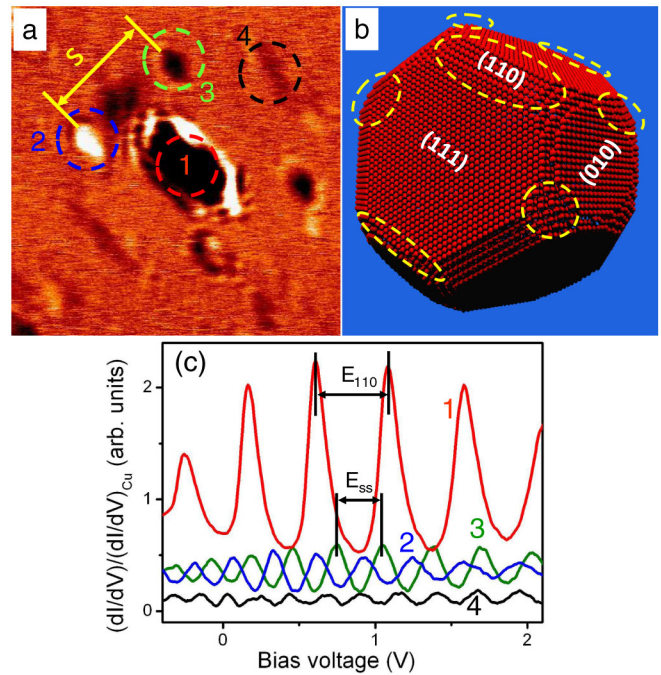


FIG. 2 (color online). (a) A typical example of the central and satellite spots in the SDC map of $20 \times 20 \text{ nm}^2$. The color of the satellite spots can be different from spot to spot and varies with the bias voltage. (b) The side view of the faceted nanocavity. The (110) facet (encircled) parallel to the surface induces the central spot. Other locations inducing the satellite spots are also encircled. (c) Plots of dI/dV measured in the marked points of (a) and normalized on $(dI/dV)_{\text{Cu}}$ at unperturbed Cu surface. Curves 2–4 are shifted vertically.

satellite spots [Fig. 2(a)] and the depth differences $\delta = d_{\text{ss}} - d_{110}$ between the upper (110) facet and the interface scattering structure has been done. The difference δ is derived from the period of SDC oscillations ΔE [Fig. 2(c)] in the central ($d_{110} \sim 1/\Delta E_{110}$) and satellite ($d_{\text{ss}} \sim 1/\Delta E_{\text{ss}}$) spots. Applying the analysis to different nanocavities, we have found that the ratio s/δ is not dependent on the depth of the upper facet, as checked for depths ranging from 2 to 10 nm. Thus, we conclude that s is proportional to the same characteristic of the nanocavity as δ , namely, the nanocavity size. This analysis confirms that the positions of the satellite spots correspond to a vertical projection of the interfacial scattering structure at the interface.

Taking into account the faceted shape of the nanocavity and the aforementioned analysis, the two elongated satellite spots are attributed to scattering at the edges of $\{111\}$ facets. These edges are parallel to the surface providing an equal phase of the electron wave. Thereby, the appearance of spots corresponding to those edges could be expected indeed. In contrast, the scattering on other inclined edges of various facets does not contribute to an observable variation of SDC. Surprisingly, and contrary to the foregoing argument, we will next show that the four small

satellite spots do correspond to an *inclined* part of the nanocavity interface.

To find out how some of these inclined interfaces may contribute to spots in the SDC whereas the others do not, we performed computer simulations of the conductance maps with a simple backscattering code. Our model description considers electron wave propagation, scattering from the nanocavity, and interference at the surface, probed with the STM, in the same way as done in previous work [6]. The propagation takes into account the band structure of Cu as well as the focusing effect providing a strong angular dependence of the amplitude of electron waves, that consistent with other studies [1,9], but done in a simplified way [6]. Because the characteristic distances of electron propagation in our system are 1 order of magnitude larger than the DeBroglie wave length, this simplified approach is reasonable. However, in order to account for diffraction effects, the previous model [6] was modified including an atomic structure at the interface of the nanocavity via a spatial modulation of the scattering potential exactly at the positions of the fcc crystalline lattice of Cu. Additionally, our model deals with a more realistic shape of the nanocavity than used previously, considering both the low-index atomically flat facets, like $\{001\}$, $\{110\}$ and $\{111\}$, and the high index adjacent areas between them. Multiple reflections are also taken into account.

Figures 3(a)–3(c) present three examples of the scattering interface as projections on the surface showing the first atomic layer of Cu around the nanocavity. The different shapes correspond to a different anisotropy of the interface energy. The simulation of SDC maps is depicted below each corresponding nanostructure Figs. 3(d)–3(f). As clearly visible, satellite spots similar to those observed in our experiment appear only for the particular shape presented in Fig. 3(b). The central spot is the result of electron reflection by the $\{110\}$ facet, which is shrunk in the other two cases [Figs. 3(a) and 3(c)]. As suggested before, the elongated satellite spots are indeed induced by the edges of the $\{111\}$ facets parallel to the surface. The four satellite spots [one is encircled in Fig. 3(e)] are induced by the ordered atomic structure in between the $\{110\}$ and $\{001\}$ facets [one is encircled in Fig. 3(b)]. A zoomed side-view of the ordered atomic structure is presented in Figs. 3(g)–3(i) for slightly different shapes at the connection of the $\{011\}$ and $\{010\}$ facets; either via introducing a small $\{021\}$ nanofacet [Fig. 3(i)], or via a direct connection [Fig. 3(g)]. Figure 3(h) presents the atomic structure encircled in Fig. 3(b). In all three examples a particular atomic structure with periodicity of $a = 0.36$ nm along $\langle 100 \rangle$ is formed by one, two, or three atomic chains forming the angle of $\varphi = \pi/4$ in respect to $[110]$. Considering the DeBroglie wavelength of the electrons of $\lambda \approx 0.50$ nm in the $\langle 110 \rangle$ direction, one can find that the diffraction condition $a \sin(\varphi) \approx \lambda/2$ is almost satisfied within the reported

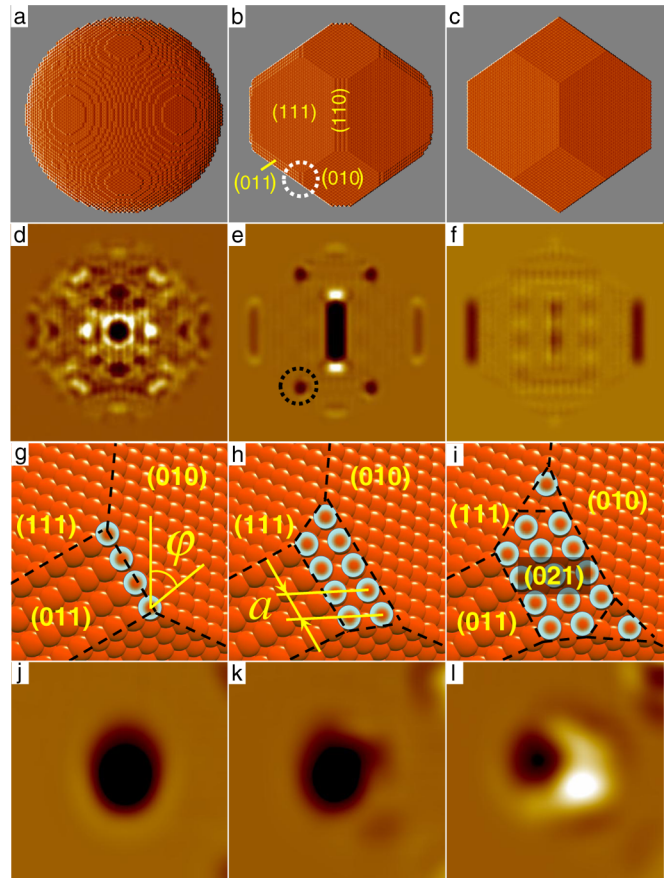


FIG. 3 (color online). (a)–(c) Different shapes of a subsurface nanocavity, represented by the first atomic layer of Cu at the interface, top view. (d)–(f) SDC maps (20×20 nm²) simulated with the model and corresponding to (a)–(c), respectively. The dashed encircling in (b) indicates the specific location of the atomic arrangement inducing the corresponding satellite spot encircled in (e). (g)–(i) Side view of the diffracting atomic structure: (h) corresponds to the encircled location in (b), and (g)–(i) are the same for slightly different shapes of the nanocavity. (j)–(l) Simulation of a satellite spot (one from the four) induced by the corresponding structure in (g)–(i), respectively. The scale of SDC maps in (j)–(l) is of 4.5×4.5 nm².

range of bias voltages. Thus, the electron diffraction from the ordered structure is responsible for the formation of the satellite spots. We emphasize that, in spite of the angular broadening of the diffracted wave and slide variation of the diffraction angle, the focusing effect [1,9–14] significantly enhances the intensity of the electron wave mainly in the $[110]$ direction.

Our simulation shows that one or two atomic chains of a few atoms each induce a satellite spot [Figs. 3(g) and 3(h)] that roughly corresponds to the experimental observation, whereas larger nanostructures usually do not provide a satisfactory match to our experiment. Thus, to agree with our experiments, the real diffracting nanostructure has to be quite short and narrow. As a consequence, the resonances are detectable in a wide range of bias voltage.

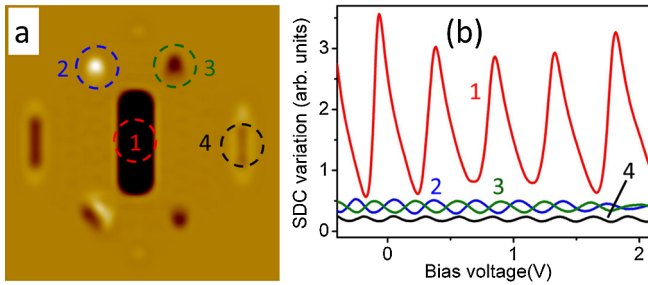


FIG. 4 (color online). (a) Simulated SDC map ($20 \times 20 \text{ nm}^2$) induced by a nanocavity with a slight shape asymmetry and distorted from one side. (b) Simulated variation of SDC in the locations encircled in (a). The curves are shifted vertically.

Usually it would also give rise to a wide angular distribution of backscattered electrons. However, thanks to the focusing effect, we observe small, well focused satellite spots, even for diffracting structure buried several nanometers below the surface.

The last issue to be addressed in this Letter is a phase difference of SDC within the four satellite spots [Fig. 2(c), curves 2 and 3]. The phase shift is attributed to an asymmetry of the nanocavity. An ideal nanocavity can be filled only with a “magic” number of atomic volumes, whereas other numbers should result in a slight asymmetry. Moreover, a statistical variation of the shape of different nanocavities is expected. As a result, the different facets are not necessarily equivalent in size leading to a slight variation of the depth and length of the diffracting chains. It should be noted that the shift of a diffracting chain to the closest neighboring atomic position leads to the phase altering by π , and thereby to a full reversal of the contrast. We performed such a simulation (Fig. 4), introducing a slight asymmetry of the nanocavity by adding one atomic layer to a few facets. The strong asymmetry at one side of the nanocavity is also realized by increasing one of $\{021\}$ facets. The resulting simulated pattern [Fig. 4(a)] nicely resembles the experimental one presented in Fig. 2(a). The calculated SDC in the central and satellite spots [Fig. 4(b)], also shows the features, observed in the experiment [Fig. 2(c)]. For example, the oscillation in the central spot reveals the narrowing of the peaks and their asymmetry, which are a fingerprint of multiple reflections in a QW. The oscillations corresponding to the satellite spots show the opposite phase as discussed above. However, the envelope of oscillations observed in the experimental plot

[Fig. 2(c)] is not well reproduced. We conjecture that this discrepancy may originate from factors neglected in the model, but fully resolving this is beyond the scope of our present Letter.

In conclusion we demonstrated that the electron diffraction on a specific, ordered subsurface structure can influence the LDOS even if the structure is inclined with respect to the surface. The focusing effect and the limited size of the diffracting structure play an important role to induce the spots of oscillating SDC in a wide range of electron energies. More generally, our results are envisioned to fuel new applications of the STM technique for a detailed characterization of subsurface nano-objects.

This work was supported by the Dutch foundation for the Fundamental Research on Matter (FOM). The authors are thankful to Martin Wenderoth and Wim de Jonge for fruitful discussions.

-
- [1] A. Weismann, M. Wenderoth, S. Lounis, P. Zahn, N. QuaaS, R.G. Ulbrich, P.H. Dederichs, and S. Blügel, *Science* **323**, 1190 (2009).
 - [2] M.F. Crommie, C.P. Lutz, and D.M. Eigler, *Nature (London)* **363**, 524 (1993).
 - [3] M.F. Crommie, C.P. Lutz, and D.M. Eigler, *Science* **262**, 218 (1993).
 - [4] M. Schmid, W. Hebenstreit, P. Varga, and S. Crampin, *Phys. Rev. Lett.* **76**, 2298 (1996).
 - [5] M. Schmid, S. Crampin, and P. Varga, *J. Electron Spectrosc. Relat. Phenom.* **109**, 71 (2000).
 - [6] O. Kurnosikov, O. A. O. Adam, H. J. M. Swagten, W. J. M. de Jonge, and B. Koopmans, *Phys. Rev. B* **77**, 125429 (2008).
 - [7] O. Kurnosikov, J. H. Nietsch, M. Sicot, H. J. M. Swagten, and B. Koopmans, *Phys. Rev. Lett.* **102**, 066101 (2009).
 - [8] I. B. Altfeder, K. A. Matveev, and D. M. Chen, *Phys. Rev. Lett.* **78**, 2815 (1997).
 - [9] Y. S. Avotina, Y. A. Kolesnichenko, S. B. Roobol, and J. M. van Ruitenbeek, *Low Temp. Phys.* **34**, 207 (2008).
 - [10] J. Heil *et al.*, *Phys. Rep.* **323**, 387 (2000).
 - [11] J. Heil, M. Primke, A. Bohm, P. Wyder, B. Wolf, J. Major, and P. Keppeler, *Phys. Rev. B* **54**, R2280 (1996).
 - [12] J. Heil, M. Primke, K. U. Wurz, and P. Wyder, *Phys. Rev. Lett.* **74**, 146 (1995).
 - [13] M. Dahne-Prietsch and T. Kalka, *J. Electron Spectrosc. Relat. Phenom.* **109**, 211 (2000).
 - [14] F. J. Garcia-Vidal, P. L. deAndres, and F. Flores, *Phys. Rev. Lett.* **76**, 807 (1996).